

MORPHODYNAMIC RESPONSE TO HUMAN ACTIVITIES IN THE BAY OF CÁDIZ (2012-2015)

Zarzuelo C¹, Diéz-Minguito M¹, D'Alpaos A², Carniello L³, Rosal-Salido J¹, Ortega-Sánchez M¹

The morphology of the Bay of Cádiz in the southwestern Spain has been changing for the past 25 years in response to the human interventions. Since 2012, new interventions, for example the new terminal and the new navigation channel, have been planned to carry out inside the Bay. As a result of these interventions, there has been a decrease in tidal amplitudes, tidal volumes, and average flow velocities, and there is hardly any sediment transport along the bay. Recent human activities are addressed in the Bay of Cádiz, an estuary located in the south-west of Spain. The Bay of Cádiz is a highly altered embayment in which socio-economical developments and ecological interests conflict. This work studies both through observations and numerical simulations the impact of some of these modifications on the morpho-hydrodynamics of the Bay of Cádiz. The capability of the bay to transport sediment between the inner and outer bay deteriorates after the deepening of the navigation channel and the construction of the new port terminal and the new bridge. This may have an impact on the ecological status of the bay. The influence of the dredging and the new terminal are concentrated at the entrance to the central sector of the bay and close to the channel. The dredging would increase siltation in the shallower areas close to the new channel, which subsequently reduce the amount of sediment input into the basins. The bridge mostly affect the Puntales Channel and the inner bay. The most changes in the erosion/deposition patterns are found in the area with strong bottom frictions and tidal asymmetries.

Keywords: Morphological evolution; human interventions; Bay of Cádiz

INTRODUCTION

Bays are large bodies of water connected to the open ocean or sea and usually formed by two portions, the outer and inner basins, which are usually fed by the small rivers, streams and tidal creeks. The shallow-water systems are mainly dominated by tidal asymmetries, which are generated by nonlinear processes of interaction. These effects promote a net flow of sediment in the direction of such asymmetries (Aubrey and Speer, 1985; Aldridge, 1997). Bays are becoming more important in modern society, due to their strategic locations and unique natural environments. Many estuaries worldwide have been modified in the past decades, in order to reclaim land and to allow even larger ship access to inland waterways. While it is highly profitable, environmental problems may also come if proper management decisions are not taken. The channel deepening and straightening as well as reclamation of the intertidal area have been some of the most popular interventions. The tidal amplification, the changes of the erosion/deposition patterns, the increasing estuarine circulation, and the increasing tidal asymmetry are some poorly known examples of the effects caused by anthropogenic influences.

Among the different anthropogenic activities at these environments, navigation and dredging, urban occupation, and marsh reclamation for accommodating new infrastructures have stronger influences on the hydro- and morphodynamics (Knowles and Cayan, 2004; Lu et al., 2009; Barnard et al., 2013; Van Maren et al., 2015). They also add complexity to the understanding of the main physical drivers of water circulation (Valle-Levinson and Blanco, 2004; Carniello et al., 2005; Zhong and Li, 2006; Valle-Levinson, 2008; D'Alpaos et al., 2010) and mixing (Walters et al., 1985; Hetland and Geyer, 2004; Burchard and Hofmeister, 2008; Venier et al., 2014). Despite the advances achieved during recent years, the assessment and prediction of present and future impacts on the hydrodynamics of bays are still challenging tasks for both managers and scientists (Li et al., 2014).

Since 2012, the Bay of Cádiz (SW Iberian Peninsula) has changed dramatically as a result of human activities. "La Pepa" Bridge, one of the longest (5 km) and highest (69 m over mean sea level) bridges of Europe, was completed in 09/24/2015. It crosses the Puntales Channel connecting the city of Cádiz with the Peninsula (see Figure 1). A new container terminal (which increases 22.5% the port surface) is under construction at the Port of Cádiz; when finished, $3.6 \cdot 10^6 \text{ m}^3$ of sediment will be dredged to shift and deepen the current navigation channel. However, the expected impacts of these interventions on the water and sediment exchange in the whole estuarine area have not been assessed on a subtidal/morphodynamics time scale.

¹Andalusian Institute for Earth System Research, University of Granada, Spain

²Department of Geosciences, University of Padova, Italy

³Department ICEA, University of Padova, Italy

In this contribution, we present the results of the analysis of the potential impacts of these ongoing interventions on the water exchange and erosion/sedimentation rates. The analysis is based on water elevation, current, and suspended sediment concentration measurements recorded during a 40-days field survey, and also on the simulation scenarios performed with a sand-mud transport model (Carniello et al., 2012).

FIELD SITE

The Bay of Cádiz is a low-inflow, dynamically short and tidally driven estuary. Tides are semidiurnal, being the M2 (12.42 hours) the main tidal constituent. The tidal range is mesotidal with typical values during neap and spring tides of ≈ 1 m and ≈ 4 m, respectively, and the water levels and currents are in quadrature (Zarzuelo et al., 2016). Tidal currents continually entrain and rework sediment with an enhancement during spring tides.

The Bay of Cádiz can be divided into two basins (inner and outer bays) that are connected through a constriction: The Puntales channel (Zarzuelo et al., 2015). Three well-defined areas can thus be identified: a deeper outer area connected with the open sea (labeled as A in Figure 1), a shallower inner one (C-Figure 1), and the Puntales channel (B-Figure 1). The Natural Park of the Bay encompasses a 10,522 ha flat landscape of sandy beaches, marshes, salt pans, freshwater lakes and tidal inlets, as well as the two natural areas of Isla del Trocadero and the Sancti-Petri and Carraca creeks (Figure 1).

The outer bay (A-Figure 1), which is affected by waves, tidal currents, and freshwater discharges during the wet seasons, extends 70 km² with an average depth of 15 m and a mean slope of 1.5 ‰. Sandy bottoms (90 %) and rocky shores and cliffs (10 %) characterize this area (Sánchez-Lamadrid et al., 2002). The San Pedro and Guadalete rivers flow into this area (Figure 1), and their discharges are mainly controlled by upstream dams.

The Puntales channel (B-Figure 1) constricts the water exchange, and harbors most of the Port of Cádiz infrastructures. The channel is 3.8 km long and 1.3 km wide, and its principal axis is oriented 33° anti-clockwise from the North. Depths in the main channel range from 11 to 15 m with maximum values of 18 m below mean low water. Mean slope in B attains a value of 9 ‰. The larger slopes (15%) in the Bay are reached at the southern end of the strait.

The inner Bay (area C in Figure 1) shows a maximum depth of 8 m and mean slopes of 2 ‰, which allow for extensive muddy intertidal flats. Nowadays, area C extends 50 km², although substantial extensions of marshes have been lost due to human activities. Bottoms are predominantly muddy (97%). A dense tidal channel network flow into this part, being Sancti-Petri and Carracas creeks the main tidal channels. The northern part is connected to the inner part of the Bay of Cadiz at La Carraca, and the southern part is connected to the Atlantic Ocean at Sancti-Petri. It has many secondary channels that feed a very complex system of small channels with large areas of marshes. Their mean depths varies from 9 m at the seaward boundary to 3 m at the inner bay boundary.

The creeks are located at the south of the bay connected with the inner bay. Sancti-Petri and Carraca creeks are very shallow domains subjected to the bay's tidal dynamics and forms part of the coastal marsh system of the Cádiz Bay Natural Park. Sancti-Petri creek has an extension of 170 ha, and comprises intertidal flats around the fringes, expanses of subtidal flats (to 2 m deep) and deeper channels (6–8 m) that discharges to the Atlantic Ocean. This reach of the tidal creek is roughly funnel shaped and is surrounded by intertidal flats, where the maximum depth is 5 m. The water column is typically well-mixed. The highest values of concentration of suspended particulate are found Sancti-Petri tidal creek (13 mg/L). The sediments in the creeks are predominantly muds, since this area is protected from winds and waves.

METHODOLOGY

Field Survey

Eight instruments were deployed at seven moorings stations from December 22, 2011 to April 18, 2012. They consisted on 4 current meters (hereinafter ADCP) and 3 tidal gauges, denoted by I1-I4 and T1-T3, respectively (black and red crosses, respectively, in Figure 1). The location of the instruments were based on the closeness with the new bridge "La Pepa" (36.52°N;6.27°W) and the new port terminal (36.54°N;6.27°W). Moreover, the instruments were located there to study the possible impacts on the water exchange between the inner and the outer bay.

The observed data were sea level and currents, which were used to evaluate water circulation and sediment transport within the bay and, in particular, the water exchange between the inner and outer basins on intratidal and subtidal-morphodynamic time scales (see Zarzuelo et al. (2015) for further details). Measurements revealed that the estuary is short tidally-driven, and elevations and currents are in quadrature.

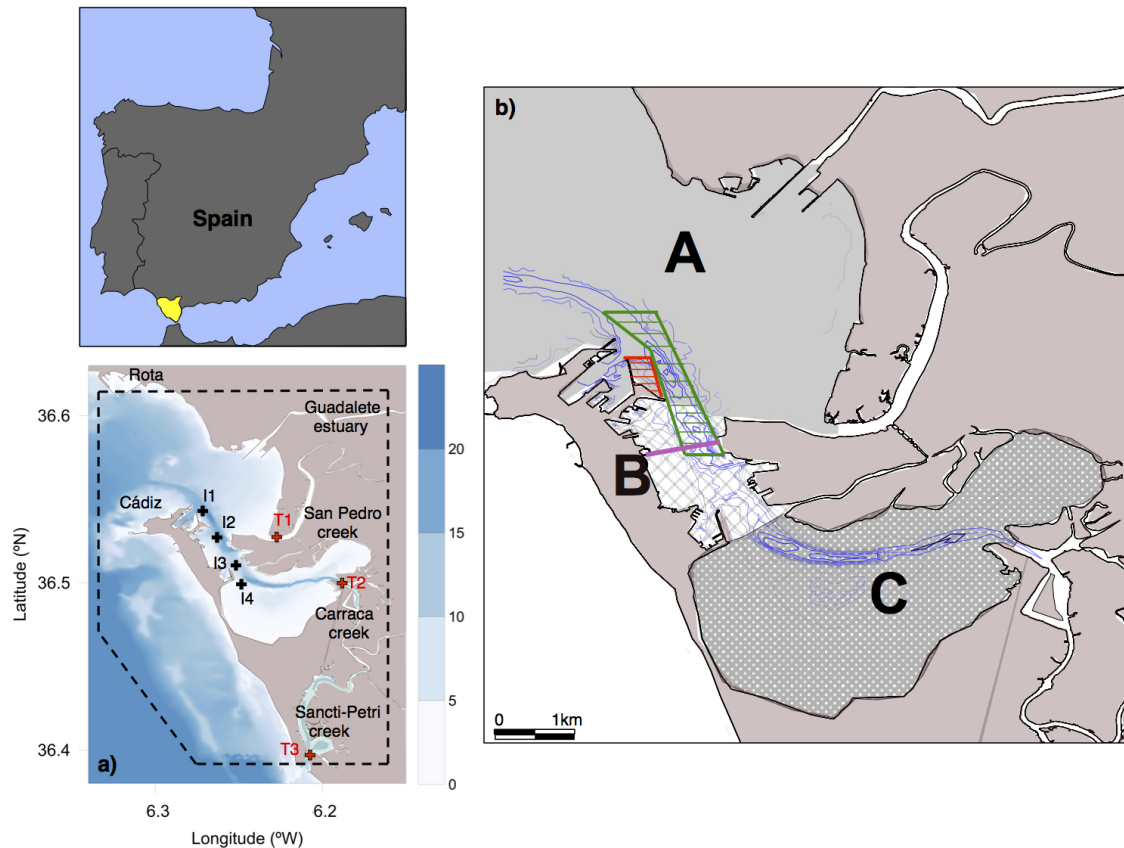


Figure 1: Panel a–Location of the Bay of Cádiz. Labels I1-I4 correspond to current profile meters, and labels T1-T3 to tidal gauges, black and red crosses, respectively. Dashed line corresponds to the boundary of the mesh. **Panel b**–Shaded areas are the outer (marked as A), central (B), and inner (C) bays. Red, green and pink shaded areas correspond to the interventions: The new terminal, the new navigation channel and the new bridge, respectively.

Model

The morphodynamic model is made up by two modules: i) a hydrodynamic module coupled with a wind-wave tidal module (hereinafter WWTM), developed by Carniello et al. (2005, 2011) and calibrated and tested for the Bay of Cádiz field site using the observed data described above, and ii) a sediment transport and bed evolution module (hereinafter STABEM) developed by Carniello et al. (2012). The election of this model was due to the capability of this model to deal with flooding and drying in very irregular domains, as is the case of Bay of Cádiz. The two modules are briefly described in the following.

The hydrodynamic module solves the two-dimensional shallow water equations and includes a refined sub-grid modeling of the bathymetry to deal with wetting and drying processes in very irregular domains. The two-dimensional shallow water equations are solved using a semi-implicit staggered finite element method based on Galerkin's approach (the reader is referred to Defina (2000) and D'Alpaos and Defina (2007) for further details). The hydrodynamic module yields tidal levels which are used by the wind-wave model to assess parameters (e.g. wave group celerity, time varying water depth) influencing on wave generation and propagation (Carniello et al., 2011).

The wind-wave module uses the parameterized approximation of the wave action conservation equation (Hasselmann, 1973) parameterized using the zero-order moment of the wave action spectrum in the frequency domain (Holthuijsen et al., 1989). The spatial and temporal variations of the wave period are estimated with an empirical correlation function, which relates the mean peak wave period to the local wind speed and water depth following the approach suggested by Young and Verhagen (1996). WWTM further considers the spatial heterogeneity of the wind field implementing the interpolation technique of the available wind data proposed by Brocchini et al. (1995) (see Carniello et al. (2011) for further details). The WWTM and STABEM have been widely tested by comparing model results to hydrodynamic, wind-wave and turbidity data collected in the Venice lagoon (Defina et al., 2007; Carniello et al., 2011) and in the lagoons of the Virginia Coast Reserve, USA (Mariotti et al., 2010).

The sediment transport and bed evolution module (STABEM) considers mixtures of sand and mud (sum of clay and silt, Carniello et al., 2012) and distinguishes between both types of sediments using them to characterize the bed composition and behaviour (cohesive or not cohesive). The transition between cohesive and non cohesive sediments is mainly determined by the mud content which varies in space and time, updated by the model on the base of the local entrainment and deposition.

STABEM solves the advection diffusion equation and the Exner equation for each class of sediment (sand and mud) coupled with WWTM. The combination between hydrodynamic and morphodynamic processes is made 'in line', i.e. bed elevation and composition are updated each time step but the option of introducing a morphological factor to speed up the morphological evolution is available in the code. Furthermore, the comparison with suspended sediment retrievals derived from the analysis of satellite images enabled us to assess the ability of STABEM to reproduce observed spatial patterns of suspended sediment concentration during storm events (Carniello et al., 2014) and to statistically characterize the spatial and temporal dynamics of resuspension events (Carniello et al., 2016). We refer the reader to Carniello et al. (2012) for further details.

Calibration and testing

The numerical simulations presented herein were carried out within a computational domain which was suitably set up to predict the tidally induced circulation in shallow basins such as the Bay of Cádiz. To run the model, a computational grid was defined on the basis of accurate bathymetric and topographic data (Figure 1). The grid consists of 31367 nodes and 62105 triangular elements of different size (smallest size about 10 m, larger element size about 80 m). The time step for the computation was set equal to 2 s. The bathymetric data were provided by the Instituto Hidrográfico de la Marina (Spanish Ministry of Defence) and the Port Authority of Cádiz. In areas where multiple data sets overlapped, preference was given to the higher resolution multi-beam data (Hansen et al., 2013).

The WWTM module was calibrated and tested using the field data. A four-step approach (Zaruelo et al., 2015) was followed to ensure accurate results. First, boundary conditions consisted on tidal levels imposed at the seaward boundary and spatially uniform winds. The tidal levels were defined with the amplitudes and phases of the twelve dominant components provided by the Oregon State Tidal Prediction Software (OTPS) (Egbert and Erofeeca, 2002), using the tools developed by Pawlowicz et al. (2002). The uniform wind data were provided by Puertos del Estado (Spanish Ministry of Public Works). Second, the model was run and calibrated at stations I1 and I3 (Figure 1), modifying the Strickler bed roughness coefficients. Finally, the model performance was checked comparing the results of the model with the observations at I1-I4 and T1-T2 (Figure 1).

The period from January 17 to January 26, 2012, was selected to calibrate the model. For this period of time, the influence of wind and waves on tidal circulation was negligible (wind speed always lower than 4 m/s). An excellent agreement between the observed and simulated tidal levels were achieved (correlation coefficient $R = 0.99$) considering the selected no-wind conditions. The regression coefficient and skill values (Olabarrieta et al., 2011) for the tidal currents are lower, but the agreement is still very good ($R = 0.94, S = 0.9$).

Once calibrated, the model was tested considering the data collected in the period from February 02 to March 14, 2012. The high values of the skill parameter (Table 1), lower for the eastern currents, indicated that the model is able to accurately reproduce the tidal dynamics of the Bay of Cádiz. Furthermore,

	tidal level (m)			East Velocity (m/s)			North Velocity (m/s)		
	<i>RMSE</i>	<i>R</i>	<i>S</i>	<i>RMSE</i>	<i>R</i>	<i>S</i>	<i>RMSE</i>	<i>R</i>	<i>S</i>
I_1	0.080	0.99	0.99	0.099	0.87	0.83	0.110	0.96	0.91
I_2	0.070	0.99	0.99	0.087	0.91	0.91	0.160	0.94	0.93
I_3	0.100	0.99	0.99	0.260	0.69	0.67	0.330	0.77	0.51
I_4	0.120	0.99	0.99	0.090	0.79	0.71	0.100	0.93	0.85
T_1	0.820	0.82	0.67	-	-	-	-	-	-
T_2	0.560	0.87	0.80	-	-	-	-	-	-

Table 1: Root mean square errors (*RMSE*), correlation coefficients (*R*) and skill coefficients (*S*), for the testing period of the elevations and velocities at I_1 , I_2 , I_3 , I_4 , T_1 and T_2 . T_1 and T_2 only measured tidal level, thus there are not measurements of velocity.

the residual currents and tidal prism was also calibrated with a good agreement ($R \sim 0.73$, table 2). Finally, the suspended sediment concentration was analyzed at station I_3 . The agreement between computed and measured values is lower than for the others variables. Notwithstanding, in view of the much more challenging task related to the description of sediment transport processes the agreement was quite good can be considered satisfactory ($R \sim 0.65$, Table 2).

	Residual Current (m/s)			water exchange (m^3)			SSC (mg/l)		
	<i>RMSE</i>	<i>R</i>	<i>S</i>	<i>RMSE</i>	<i>R</i>	<i>S</i>	<i>RMSE</i>	<i>R</i>	<i>S</i>
I_3	0.04	0.79	0.8	1.01	0.74	0.73	24.1	0.66	0.65

Table 2: Root mean square errors (*RMSE*), correlation coefficients (*R*) and skill coefficients (*S*), for the calibration period of the residual currents, the water exchange and the suspended sediment concentration at I_3 .

Definition of model scenarios

To analyze the influence of the recent human interventions in the hydrodynamics and sediment dynamics of the estuary, different scenarios were defined:

Scenario 1 (Sc_1): Configuration of the Bay in 2012, before interventions. This first scenario corresponds to the configuration of the Bay of Cádiz before any intervention carried out recently (upper left panel in Figure 1). This corresponds to the bathymetric data described in section 4.1 and the configuration during the field measurements. Both numerical models have been calibrated and tested for this scenario.

Scenario 2 (Sc_2): Configuration of Sc_1 including the new port terminal and navigation channel. Those interventions are expected to be finished by the end of 2016. The coastline of zone A will be expanded, whereas the bathymetry of this area will be increased 5 m in depth (P2.2 and P3.2, respectively, in Figure 1–upper right panel). The new container terminal is characterized by a length of 590 m, forming an area of 380,000 m^2 with a maximum depth of 16 m. Additionally, the operational scheme for the new terminal includes a significant dredging of $\sim 3.86 \cdot 10^6 m^3$ to achieve a maximum depth of 20 m (new navigation channel). Accordingly, both the coastline and bathymetry of Sc_1 were adapted to include those changes. Delft3D model was used to simulate the hydrodynamics, whereas model by Carniello et al. (2012) simulate the morphodynamics.

Scenario 3 (Sc_3): Configuration of Sc_1 including the new bridge. "La Pepa" Bridge was completed on september, 2015. It is one of the longest (5 km) and highest (69 m over mean sea level) bridges of Europe, and crosses the Puntales Channel connecting the city of Cádiz with the Peninsula. Its affection on the Bay is mainly due to the nine piers set in the water that sustain the bridge (see Figure 1–lower

left panel). Carniello et al. (2012) model is used to simulate this scenario; due to the small scale of the piers, it is important that the mesh of the model around the bridge can describe these elements accurately. Hence, the mesh is intensified around the piers adding 39509 triangle nodes and 78389 triangular elements. Alongside the bridge, the node distances arrange gradually from 5 to 20 m.

Scenario 4 (Sc₄): Expected configuration of the Bay after all interventions are finished –(Sc₁+Sc₂+Sc₃)–

.This scenario represents the combination of all the interventions into a unified scenario, which will correspond to the future and final configuration of the Bay of Cádiz (Figure 1, lower right panel) by the end of 2016. Carniello et al. (2012) model is used to simulate this scenario considering all the particularities previously specified.

RESULTS

Residual Transport

Residual transports are caused by multiple factors, ranging from nonlinearities in the bed stress, continuity equation, and advection term in momentum equation, to irregular topography. Residual currents are estimated by time-averaging over each tidal cycle. Before the interventions, the residual currents are, in general, one order of magnitude lower than the tidal currents. Larger values (≈ 0.3 m/s) are observed in the mouth of the San Pedro estuary. Other local maxima occur at the Carracas Creek and along the channel where the bathymetry deepens and there are abrupt changes in the bathymetry. Panels a1-c1 in the Figure 2 shows the variations in the magnitudes of the residual currents after the different interventions ($|\bar{U}_{Sc_{2,3,4}}| - |\bar{U}_{Sc_1}|$).

Scenario 2: As shown in panel a1 in Figure 2, the effects of the dredging and new terminal on the residual current magnitude are apparent, tend to decrease respect to the values of Sc₁ in the inner and central portion of the bay (25% and 35%, respectively). The greatest increase occur near the new terminal (25%). Moreover, the increase is strongest between the channel and the inner portion of the bay (5%).

Scenario 3: Panel b1 in Figure 2 shows the effects of the residual current due to the new bridge. The changes are arranged along the SW waterway at the Puntales Channel, which are all formed under the influence of topography. The maximum decrease (20%) inside the bay is caused by low current. The maximum changes occur near to the bridge. Residual transports increase slightly after the bridge construction (15%).

Scenario 4: The residual transport in the last scenario (panel c1-Figure 2) changes along the navigation channel at the inner bay, with a maximum decrease of 35%. The maximum increase is found around the new terminal (20%).

An increase (decrease) in the velocity of the water may cause erosion (sedimentation) processes. The changes from erosion to sedimentation, or vice versa, will be determined by the direction of residual currents, it will be discussed in the next section. Nevertheless, the real storage of sedimentation will depend on sediment availability.

Mud sediment concentration (MSC)

The sediment transport changes depending the tide, causing erosion and deposition. The sand and mud concentration has been analyzed at different period, for example flood and ebb tide period, however here it only appears the change at flood period, because it is when the maximum changes occurs. Before the interventions, the values of MSC are higher at ebb (up to 140 mg/l) than flood period (up to 40 mg/l). Figure 2 shows the variations in the MSC after the different interventions.

Scenario 2: The maximum variations of MSC are found at inner bay and inside the creeks at flood period (panel a2-Figure 2). The MSC is reduced up to 20% at the inner bay, this sediment could be move to the Puntales Channel, where the MSC is increased up to 50%.

Scenario 3: The concentration of the MSC increase over 10% in the inner bay (panel b2-Figure 2). This mud mainly seems to come from the mouth of the Carracas creek and the middle of the navigation channel, where there is a decrease of MSC (20%).

Scenario 4: This reference scenario assesses the future conditions of the Bay (panel c2-Figure 2). The new bridge and the sediment extraction by dredging the port has led to a pronounced decrease in MSC. The

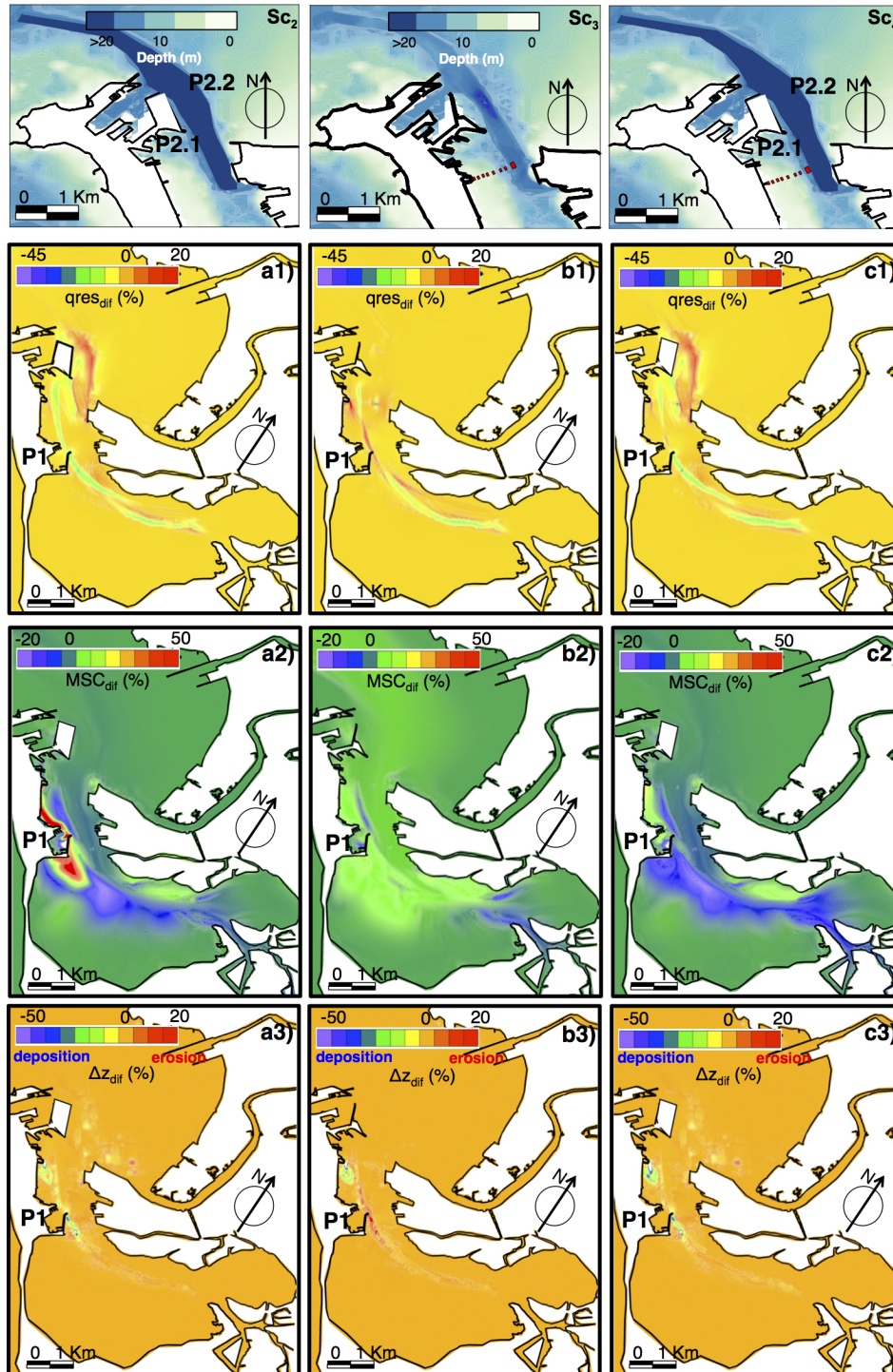


Figure 2: First row of panels correspond to the bathymetry of the different scenarios (left to right, Sc_2 , Sc_3 and Sc_4). The second row of colormaps represents the variation in the magnitudes of the residual currents (%). The third row of panels corresponds to the variations of mud concentration (%) in the Bay of Cádiz at flood tide period. Finally, a time series of bottom elevation (%) in the Bay of Cádiz at flood tide period are represented in the fourth row of panels. Panels a, b and c correspond to $Sc_{2,3,4} * 100 / Sc_1$, respectively (blue = decrease and red = increase).

inner bay is the most affected, the MSC is reduced by 20% and only is increased close to Trocadero creek and the west of the Puntales Channel (20%); this MSC could come from the inner bay.

Bottom elevation

Panels a3-c3 in Figure 2 shows the net evolution of the bottom elevation at the end of the simulation in each scenarios. Before the construction of the bridge, the southern area of the Puntales channel and the entrance of the inner bay are eroded. Due to erosion and deposition during the tidal cycle, the bottom evolves and usually organizes itself in a pattern of shallow shoals separated by deep channels.

Scenario 2: The bottom elevation (panel a3-Figure 2) is increase up to 10% at the mouth of the San Pedro estuary, which causes a erosion. In the contrary the bottom elevation is decreased up to 50% at the Puntales channel close to the new navigation channel, which causes a strong deposition. Finally, the inner bay is weakly affected by the dredging, decreasing up to 10%.

Scenario 3: The bottom elevation (panel b3-Figure 2) is increase up to 15% at the Puntales channel close to the new navigation channel, which causes a erosion. At south-west of the bridge the bottom elevation is reduced around 10%.

Scenario 4: The last scenario assesses the future conditions of the Bay (panel c3-Figure 2). The effect of the bridge is mitigating with the construction of the new channel navigation. The variations is so similar to scenario 2. There are a reduction of 50% at the Puntales channel close to the new navigation channel and increase of 10% at the mouth of the San Pedro estuary.

CONCLUSION AND SUMMARIZE

The response to these human interventions show that the dredging activity has exerted profound impacts on the morphological evolution of the embayment system: the deeper channels have experienced further erosion while the shallower shoals (ridges) have accreted further higher, and the overall stability of the embayment system has been maintained.

Major channel deepening works will alter the sediment transport regime. The influence of the construction is greater in the outer and central sectors of the bay. The influence of the dredging and the new terminal are concentrated at the entrance to the central section of the bay and close to the channel. The dredge increased siltation in the shallower areas close to the new channel, which subsequently reduced the amount of sediment input into the basins and will increase the requirement for maintenance dredging. The magnitudes and variations of suspended sediment concentrations in major channels closely follow the strengths of tidal flow. The residual currents changes and their effect on sediment erosion, deposition and transport may cause secondary geomorphological changes away from the dredge location, including the potential erosion of intertidal areas.

The comparison of the previous studies with our results shows that there are notable increases (reductions) close to the dredged area (surroundings of the dredged area). Furthermore, there are several similarities for areas where erosion and sedimentation dominate. Previous studies showed that baroclinic processes influence an estuary's suspended sediment dynamics, and the magnitude of estuarine circulation increases as a result of deepening. Over the long term, the sediment dredged from the channels may reduce the sediment concentration in the estuary. The quantity of sediment could depend on the seasonal variation or availability of sediment. Most authors agree that intertidal areas provide a natural sink for sediment to accumulate.

The influence of the bridge has been analyzed too. The bridge's influences at the Puntales Channel and the inner bay are the largest. Especially at the west of the Puntales Channel. The net variation of the bottom elevation provided by the model clearly shows the crucial role of wind waves in driving the lagoon bathymetry evolution and the net erosion of tidal flats, in particular in the central southern part of the basin. Furthermore we can observe the deposition within the main channels, which periodically need dredging.

The future development of the bay depends heavily on the future constructions. In conclusion, the interventions have a relatively large impact on the bay dynamics, which is most obvious for the tidal flow and the residual current. The results indicate that the ability of the bay to exchange water and transport

sediment between the inner and outer bay will deteriorate, thus impacting the ecological environment of the bay. For example, the changes could promote sedimentation in the inner bay because of the lower current velocities. It is suggested that (i) the main channels will become even shallower, which will concentrate the tidal currents running through them, or (ii) the shallow areas will become so deep that the tidal currents are not very effective at transporting sediment.

ACKNOWLEDGEMENTS

This work was funded by the Bay of Cádiz Port Authority and the Andalusia Regional Government, ARG, (Project P09-TEP-4630). The first author was partially funded by the ARG, Research Grant RNM-6352.

References

- Aldridge, J., 1997. Hydrodynamic model predictions of tidal asymmetry and observed sediment transport paths in Morecambe Bay. *Estuarine, Coastal and Shelf Science* 44, 39–56.
- Aubrey, D.G., Speer, P.E., 1985. A study of non linear shallow inlet estuarine system Part I: Observations. *Estuarine, Coastal and Shelf Science* 21, 185–205.
- Barnard, P., Schoellhamer, D., Jaffe, B., Lester, J., 2013. Sediment transport in the San Francisco Bay Coastal System: An overview. *Marine Geology* 35, 3–17.
- Brocchini, M., Wurtele, M., Umgiesser, G., Zecchetto, S., 1995. Calculation of a mass-consistent two-dimensional wind-field with divergence control. *Journal of Applied Meteorology and Climatology* 34(11), 2543–2555.
- Burchard, H., Hofmeister, R., 2008. A dynamic equation for the potential energy anomaly for analysing mixing and stratification in estuaries and coastal seas. *Estuarine, Coastal and Shelf Science* 77, 679–687.
- Carniello, L., D'Alpaos, A., Botter, G., Rinaldo, A., 2016. Statistical characterization of spatio-temporal sediment dynamics in the Venice lagoon. *Journal of Geophysical Research* 121 (5), 1049–1064.
- Carniello, L., D'Alpaos, A., Defina, A., 2011. Modeling wind waves and tidal flows in shallow micro-tidal basins. *Estuarine, Coastal and Shelf Science* 92, 263–276.
- Carniello, L., Defina, A., D'Alpaos, L., 2012. Modeling sand-mud transport induced by tidal currents and wind waves in shallow microtidal basins: Application to the Venice Lagoon (Italy). *Estuarine, Coastal and Shelf Science* 102–103, 105–115.
- Carniello, L., Defina, A., Faherazzi, S., D'Alpaos, L., 2005. A combined wind wave-tidal model for the Venice lagoon, Italy. *Journal Geophysical Research* 110, F04007.
- Carniello, L., Silvestri, S., Marani, M., D'Alpaos, A., Volpe, V., Defina, A., 2014. Sediment dynamics in shallow tidal basins: In situ observations, satellite retrievals, and numerical modeling in the Venice Lagoon. *Journal of Geophysical Research* 119(4), 802–815.
- D'Alpaos, A., Lanzoni, S., Marani, M., Rinaldo, A., 2010. On the tidal prism channel area relations. *Journal of Geophysical Research* 115(F1), F03001.
- D'Alpaos, L., Defina, A., 2007. Mathematical modeling of tidal hydrodynamics in shallow lagoons: A review of open issues and applications to the Venice lagoon. *Computers & Geosciences* 33, 476–496.
- Defina, A., 2000. Two-dimensional shallow water equations for partially dry areas. *Water Resources Research* 36, 3251–3264.
- Defina, A., Carniello, L., Fagherazzi, S., D'Alpaos, L., 2007. Self organization of shallow basins in tidal flats and salt marshes. *Journal Geophysical Research* 112, F03001.
- Egbert, G., Erofeeca, S., 2002. Efficient inverse modeling of barotropic ocean tides. *Journal of Atmosphere Ocean Tech.* 19, 183–204.

- Hansen, J., Elias, E., List, J., Erikson, L., Barnard, P., 2013. Tidally influenced alongshore circulation at an inlet-adjacent shoreline. *Continental Shelf Research* 33, 26–38.
- Hasselmann, K., 1973. Measurements of wind-wave growth and swell decay during the Joint North Sea-Wave Project (JONSWAP). *Dtsch. Hydrogr. Zeit. Suppl.*, 12 (A8), 1–95.
- Hetland, R.D., Geyer, W.R., 2004. An idealized study of the structure of long, partially mixed estuaries. *Journal of Physical Oceanography* 34(12), 2677–2691.
- Holthuijsen, L., Booij, N., Herbers, T., 1989. A prediction model for stationary, short-crested waves in shallow water with ambient currents. *Coastal Engineering* 13, 23–54.
- Knowles, N., Cayan, D., 2004. Elevational dependence of projected hydrologic changes in the San Francisco estuary and watershed. *Climate Change* 62, 313–336.
- Li, P., Li, G., Qiao, L., Chen, X., Shi, J., Gao, F., Wang, N., Yue, S., 2014. Modeling the tidal dynamic changes induced by the bridge in Jiaozhou Bay, Qingdao, China. *Continental Shelf Research* 34, 43–53.
- Lu, Y., Ji, R., Zuo, L., 2009. Morphodynamic responses to the deep water harbor development in the Caofeidian sea area, China's Bohai Bay. *Coastal Engineering* 56, 831–843.
- Mariotti, G., Fagherazzi, S., Wiberg, P.L., McGlathery, K.J., Carniello, L., Defina, A., 2010. Influence of storm surges and sea level on shallow tidal basin erosive processes. *Journal of Geophysical Research: Oceans* 115(C11).
- Olabarrieta, M., Warner, J., Kumar, N., 2011. Wave-current interaction in Willapa Bay. *Journal of Geophysical Research* 116, C12014.
- Pawlowicz, R., Breardsley, B., Lentz, S., 2002. Classical tidal harmonic analysis including error estimates in MATLAB using T_TIDE. *Computers & Geosciences* 28, 929–937.
- Sánchez-Lamadrid, A., Jiménez, T., Ruiz, J., Gutiérrez, G., Muñoz, J., Saavedra, M., Juárez, A., Romero, M., Pérez, A., 2002. Bahía de Cádiz Protección de los recursos naturales pesquero y aplicaciones para instalaciones Acuícolas (Consejería de Agricultura y Pesca de la Junta de Andalucía).
- Valle-Levinson, A., 2008. Density-driven exchange flow in terms of the Kelvin and Ekman numbers. *Journal of Geophysical Research* 113, C04001.
- Valle-Levinson, A., Blanco, J.L., 2004. Observations of wind influence on exchange flows in a strait of the Chilean inland sea. *Journal of Marine Research* 62, 720–740.
- Van Maren, D., Van Kessel, T., Cronin, K., Sittoni, L., 2015. The impact of channel deepening and dredging on estuarine sediment concentration. *Continental Shelf Research* 35, 1–14.
- Venier, C., D'Alpaos, A., Marani, M., 2014. Evaluation of sediment properties using wind and turbidity observations in the shallow tidal areas of the Venice Lagoon. *Journal of Geophysical Research* 119, 1604–1616.
- Waiters, R., Cheng, R., Conomos, T., 1985. Time scales of circulation and mixing processes of San Francisco Bay waters. *Hydrobiologia* 129, 37–58.
- Young, I.R., Verhagen, L.A., 1996. The growth of fetch-limited waves in water of finite depth. Part 1: Total energy and peak frequency. *Coastal Engineering* 29(1–2), 47–78.
- Zarzuelo, C., D'Alpaos, A., Carniello, L., Díez-Minguito, M., López-Ruiz, A., Ortega-Sánchez, M., 2016. Flow and sediment transport on a tidal creek influenced by ocean-bay tide. *Journal of Geophysical Research (Under Review)*.
- Zarzuelo, C., Díez-Minguito, M., Ortega-Sánchez, M., López-Ruiz, A., Losada, M., 2015. Hydrodynamics and response to planned human interventions in a highly altered embayment: The example of the Bay of Cádiz (Spain). *Estuarine, Coastal and Shelf Science* 167, 75–85.

Zhong, L., Li, M., 2006. Tidal energy fluxes and dissipation in the Chesapeake Bay. *Continental Shelf Research* 26, 752–770.